Dielectric Resonator Based MIMO Antenna System Enabling Millimeter-Wave Mobile Devices

Dielectric Resonator Based MIMO Antenna System Enabling Millimeter-Wave Mobile Devices

Mohammad S. Sharawi, Symon K. Podilchak, Mohamed T. Hussain and Yahia M.M. Antar

Abstract

In this work a millimeter-wave (mm-wave) dielectric resonator (DR) based multiple-input-multiple-output (MIMO) antenna system based on two linear arrays is presented. Each array that represents a single MIMO antenna consists of four cylindrical DR antenna (cDRA) elements operating at 30 GHz with a bandwidth of at least 1 GHz. Each array is designed with a fixed beam direction which is tilted to provide low field correlation. A passive microstrip-based feed network was designed to achieve this beam tilting enabling suitable magnitude and phase excitation of the individual cDRAs for radiation. The complete antenna system was designed on a two-layer substrate occupying 48 mm by 21 mm. Excellent field correlation values were measured (below 0.002) across the band of operation while peak gains were greater than 7 dBi. High radiation efficiency is obtained. The proposed design approach for beam tilting, which enables MIMO operation, may also be useful for other compact implementations to support 5G communications.

I. Introduction

Dielectric resonator antennas (DRAs) are well known in literature. Generally they consist of a dielectric volumetric structure that is excited via a coupling feed line. Several geometries have been devised such as hemi-spherical, cylindrical, and rectangular. Variations of these shapes have also been investigated, and the design procedures for all of these types is well documented [1]–[3]. In addition, a wide variety of dielectric materials and ceramics can be used for such DRA structures, and one can find relative dielectric constants varying between 3 and 100. Also, the higher the dielectric constant, the smaller the DRA size can become, albeit at the expense of a narrower operating bandwidth (higher quality factor, i.e. Q) and possibly higher cross-polarization levels.

The use of DRAs for millimeter-wave (mm-wave) applications has also been demonstrated. For example, a linear antenna array was proposed in [4] at 33.9 GHz. The series fed array was excited using substrate integrated waveguide technology. This mm-wave linear array achieved 90% efficiency and offered a gain of 11 dBi with four rectangular DRA elements having ϵ_r = 10.2. In [5], a 60 GHz slot coupled DRA was proposed with reported efficiencies greater than 98%. The rectangular

DRA was made of a dielectric material with ϵ_r = 12.6. The design achieved a 6.1% impedance bandwidth (BW). In [6], a linear four-element rectangular-based DRA array was also proposed offering a BW of 0.5% with an operational frequency of 40 GHz. The array was fed with a corporate, microstrip-based feed structure where the main beam was directed at broadside.

Other feeding approaches have also been published including direct DRA probe feeding at microwave frequencies and dielectric waveguide implementations for mm-waves. For example, in [7] a linear antenna array consisting of twelve, rectangular-based DRA elements was designed for operation from 32 GHz to 35 GHz. In that structure the far-field beam was tilted from broadside with a maximum angle of 20°. More recently, some DRA-based arrays were studied in [8] and [9]. In [8], a low cost phased array operating from 2.7 to 2.8 GHz was presented. The array consisted of a driven DRA and two parasitic elements which were loaded with variable capacitors to achieve beam control defining an electronically steerable passive array radiator (ESPAR). In [9], similar concepts to that of [8] were followed but with additional antenna elements and with slot coupled feeding.

Nowadays, 4G and upcoming 5G wireless systems and devices require new antenna and circuit configurations. Moreover, multiple-input-multiple-output (MIMO) antennas are a corner stone in these architectures and designing and evaluating their performance metrics is an important task that is required for future mobile terminals, advancing antenna technology, and thus leading to efficient system operation [10], [11]. However, at this stage in the development, the use of DRA-based MIMO antennas has not been widely investigated and limited works above 3.5 GHz [12]–[14] have appeared addressing these challenges.

It is clear that mm-wave MIMO DRA based designs have not been thoroughly investigated for next generation devices and similar communication applications. It has been recently reported that mm-wave bands with at least 500 MHz of BW in the 28 GHz and 38 GHz frequency bands can be used in wireless cellular communication systems [15]. High gain antenna arrays may also be required, mainly due to the fact that short range communications are needed to compensate for the large free-space path losses that can be observed in the channel. Since MIMO can also offer advantages when considering multipath effects, the combination of both DRA-based arrays and MIMO configurations can provide some novel antenna and circuit solutions for these applications at mm-wave frequencies.

In this work, we propose the first cylindrical DRA (cDRA) based, mm-wave MIMO antenna system with simple feeding and compact size for future 4G and 5G wireless terminals (see Fig. 1). The MIMO antenna system can be positioned at the edge of any mobile terminal and consists of two arrays with four elements that are closely spaced. More importantly, arrays are selected for the MIMO antenna system to compensate for the free-space path losses that can be observed at mm-wave frequencies as well as provide beam steering capability to reduce channel correlation. This can minimize the operating costs of any supporting power amplifiers and other control circuitry.

The proposed MIMO antenna system is highly efficient at mm-wave frequencies when compared to other planar implementations and similar metallic-based arrays that can suffer from noticeable surface-wave and conductor losses. From a more classic array perspective, the inter-element periodicity for the array elements is the same as illustrated in Fig. 1, making the structure appear as a standard eight element array. However, the feed system adopts intentional beam-tilting enabling low field correlations in the far-field and thus offers reduced channel correlation which is ideal for MIMO communications. Although some papers showed some orthogonal pattern behaviour for some MIMO antennas via antenna placement or pattern reconfigurability as in [16], [17], none where shown with an array configuration or for operation at mm-waves. The detailed literature review described above shows that the simple MIMO antenna design, as proposed in this paper, has not been investigated previously offering good integration, compact size, high gain, and simple fabrication for 5G mm-wave mobile handset applications.

II. Design of the mm-Wave MIMO Antenna Array

The proposed MIMO antenna is implemented using PCB technology and consists of two, four-element arrays, each with a tilted $\pm 45^{\circ}$ beam pattern. The feed network is carefully designed to provide the tilted beams from the two antenna arrays allowing for good correlation coefficient and diversity gain. In addition, the size of the cDRA-based array allows for simple integration with mobile terminals and other Wi-Fi devices and occupies 10 mm by 45 mm by 3.1 mm on the top layer while the feed network occupies 11.4 mm by 40 mm on the bottom layer. Figure 1 shows the diagram of the proposed cDRA-based MIMO antenna system for operation at mm-wave frequencies (30 GHz). Two groups of the four-cDRA elements, arranged in a linear-array, are considered as a single MIMO antenna. The individual cDRAs have a diameter and height of 3.2 mm and 3.1 mm, respectively. These element sizes were initially determined using the formulas in [1], [3] for the $\mathrm{TE}_{011+\delta}$ mode (the generated E and H-fields inside the cDRAs are shown in Fig. 1(b) and (c) for the first two elements incorporating their progressive phases, respectively). In addition, the inter-element spacing between adjacent cDRAs was 6 mm (center-to-center) and HiK500 material was used for these elements with ϵ_r = 10 and $\tan\delta$ = 0.002.

The feed network was designed and placed on the bottom layer while the cDRA array was positioned on the top system ground plane allowing for simple integration with other electronics and on-chip devices. The microstrip feed network for each array with 50-Ω and 70.7-Ω lines, occupies 11.4 mm by 20 mm, representing a conventional 4-port power divider/combiner [18] with some pre-calculated meandered microstrip lines to provide the phase shifts required. These phase shifts for each 4-element linear array were calculated using the formulas in [19] to generated a tilted beam towards +/- 45^{o}. The feeding mechanism is shown in Fig. 1. The top ground (GND) plane layer has cDRA coupling slots. The slot was centered with respect to the base of the cDRA with dimensions 1.2 mm by 1.3 mm (exploded view in Fig. 1 inset). In addition, the microstrip feed line extended 0.5 mm beyond the center point for cDRA excitation and impedance matching. The microstrip line width

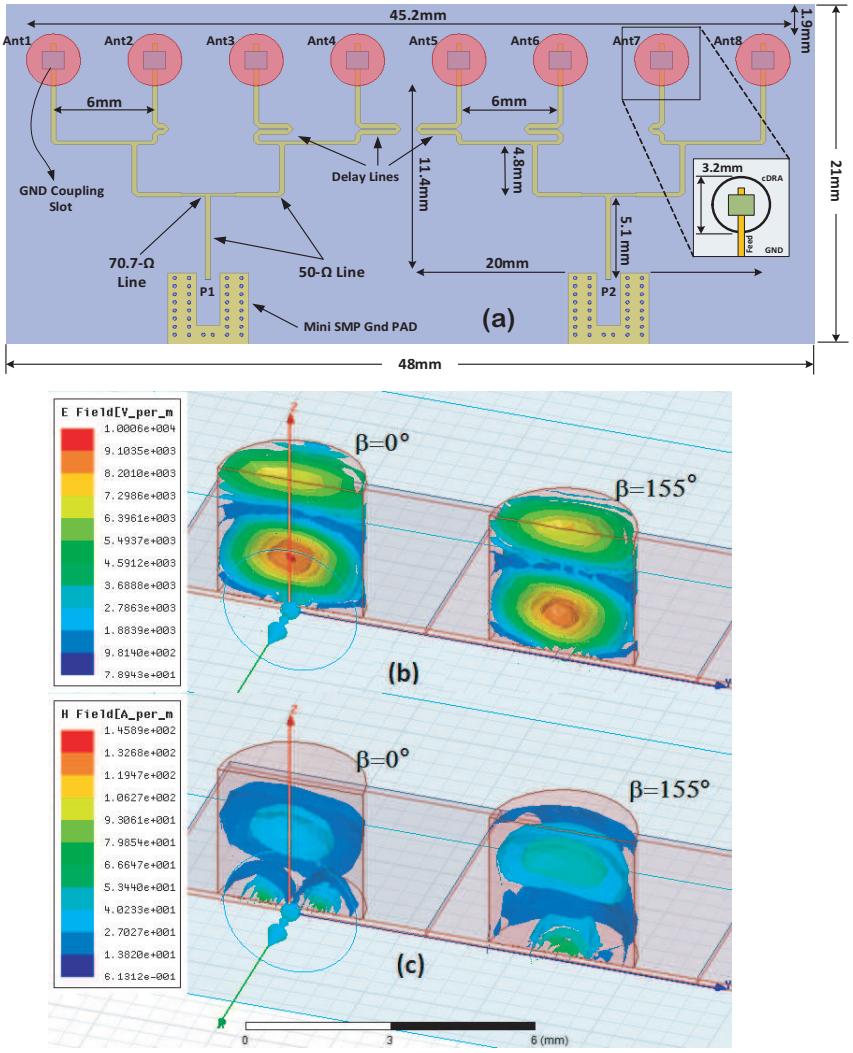

Fig. 1. (a) Layout of the mm-wave MIMO antenna array. cDRAs are on the top GND layer while the microstrip feed network is on the bottom layer. Exploded view shows the feeding mechanism for a single cDRA. All dimensions in mm. (b) shows the E-fields in DRA-1 and DRA-2, (c) shows the H-fields in DRA-1 and DRA-2.

was 0.3 mm with 50-Ω impedance and was printed on an RO3003 substrate with ϵ_r = 3, $\tan\delta$ = 0.001 having a thickness of 0.13 mm.

The feed network on the bottom layer was designed to provide appropriate phase shifts to independently tilt the beams left and right, such that $\pm 45^\circ$ elevation angle tilts were achieved in the far-field. Moreover, the feed network is expected to provide similar amplitude levels (ideally 1/4 of total as in a power splitter/combiner) and progressive phase angles of $+153^\circ$ for antenna elements 1 through 4 and -153° for antenna elements 5 through 8.

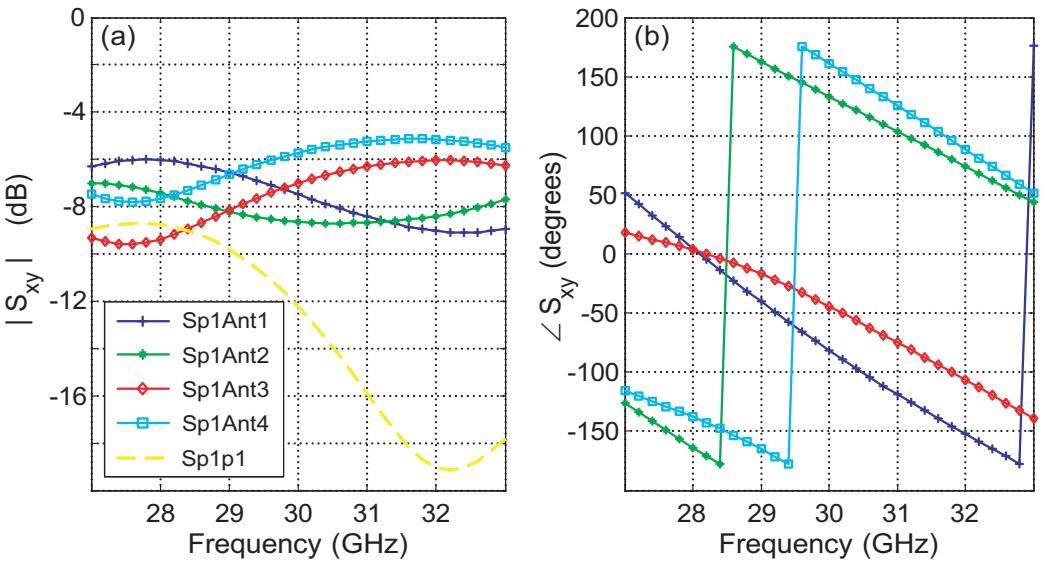

Fig. 2. Simulated S-parameters for the feed network illustrated in Fig. 1 for port 1, (a) amplitudes and (b) phases. Port 1 is the input port of the first antenna array (see Fig. 1). The insertion loss between port 1 and antenna element 1 is Sp1Ant1, and for antenna element 2 it is Sp1Ant2 and so on.

III. Results and Discussions

The mm-wave, cDRA MIMO anntenna system was modeled and optimized using HFSS^{TM}. The response of the feed network without the cDRA arrays is shown in Fig. 2. The obtained magnitude values at 30 GHz were (0.268, 0.199, 0.136, 0.178) for the four array elements (compared to 0.25 in the ideal case) and the relative phases with respect to the first antenna were (0°, 155°, -26°, 120°) for ports Ant1 through Ant4, respectively. Similar values were obtained for the other array and these amplitude and phase responses can guarantee at least 1 GHz of operating impedance BW; i.e.$|S_{xx}| < -10$ dB as shown in Fig. 4(a). Note that the magnitude errors at the feed network output did not exceed 2.3 dB (due to path lengths) while the phase error did not exceed 28° over the desired operating BW. These values affected the beam tilts a little bit (less than 5^o) as well as the side-lobe-levels (SLL) and null locations of the obtained patterns. It should also be mentioned that the inter-element spacing of the cDRA elements played a role in not being able to achieve a perfect match between the required and ideal phases for the array, however acceptable MIMO performance values were still obtained as will be shown.

The fabricated prototype is shown in Fig. 3. In particular, Fig. 3(a) shows the top layer of the fabricated cDRA based MIMO antenna array along with the rigid (backing) plastic material. The cDRAs were machined with almost equal heights of 3.05 mm each, except one which was 3.06 mm. The cDRAs were attached to the top layer using a bonding agent (glue) material with ϵ_r = 10, and an approximate thickness of 70 μm. The rigid plastic material of 0.9 mm thickness with ϵ_r = 4.0 was used on the top layer to provide mechanical strength to the 0.13 mm thin substrate. During the measurements this enabled simple connectivity of the testing cables as well as minimal bending and twisting to the compact antenna. Although the rigid

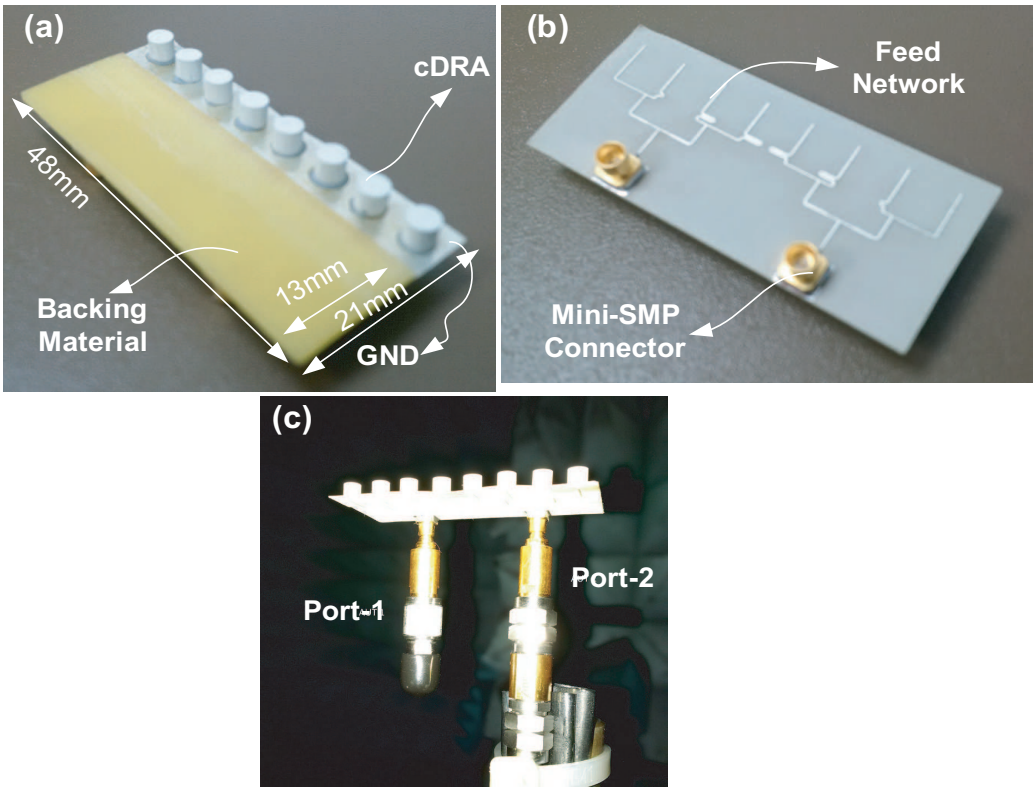

Fig. 3. Fabricated mm-wave cDRA array based MIMO antenna system, (a) top view, (b) bottom view, and (c) measurement setup.

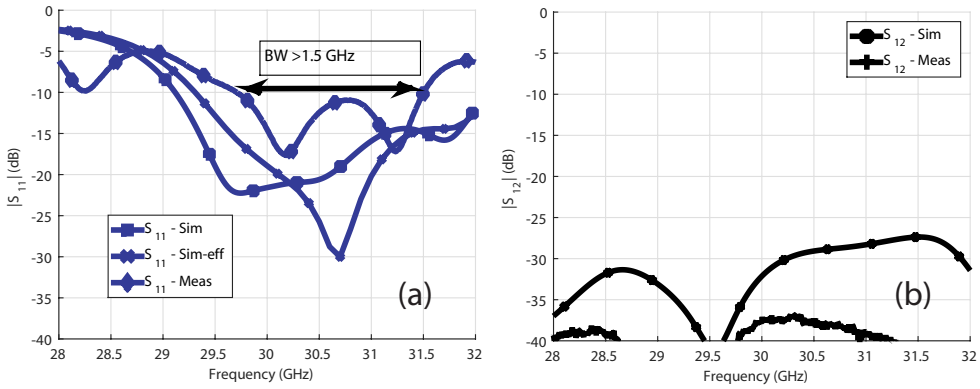

Fig. 4. Measured and simulated S-parameters for the mm-wave cDRA based MIMO antenna system, (a) reflection coefficient, (b) mutual-coupling.

material was close to the cDRAs, it did not affect their port parameters, and its edge was chamfered to minimize its effect on the radiating fields. The feed networks for both arrays with their mini-SMP connectors (PE49989) are shown in Fig. 3(b). A side view of the measurement setup showing one port connected and the other terminated with 50-Ω is shown in Fig. 3(c).

The complete system response in terms of S-parameters is shown in Fig. 4 and these measurements were completed using an Agilent N5572A PNA. The reflection coefficient for port one is shown, as the other is similar due to symmetry. Fig. 4(a) shows the simulated (sim) reflection coefficient ($|S_{xx}|$) response of the simulation model as described before with cDRA

parameters based on the actual machined dimensions. The curve (Sim-eff) shows the effect of incorporating a 2% variation in the ϵ_r $(= 9.8)$, as well as a glue height of 100 μm in the simulation model. The measured reflection coefficient curve shows acceptable agreement with the two simulated cases; i.e. similiar -10 dB impedance BWs are observed. The measured and simulated coupling curves show coupling levels that are less than -25 dB in Fig. 4(b). The discrepancy observed in the $|S_{xx}|$ curves is likely related to several fabrication issues; the first being the possible misalignment of the center coupling slot with the center of the cDRAs. Another is related to the bonding material and its thickness variation from one cDRA to another and thus affecting the effective height of the DR elements. Finally, these discrepancies might also be related to process variations in the dielectric properties of the cDRAs as well as substrate variations for the feed system.

Parametric sweeps were completed to further investigate the effects of the fabrication process on the S-parameters. One parameter was investigated while others were held constant. This is important to explain any discrepancies between the measurements and the simulations. In Fig. 5(a) the dielectric constant values of the cDRAs were swept between 9.8-10.4 in 0.2 steps, to account for 4% error in ϵ_r. Almost a 1 GHz frequency shift is noticed in the position of the $|S_{xx}|$ minimum. The effect of the cDRA diameter on $|S_{xx}|$ is also shown in Fig. 5(b). A severe mismatch is observed when the glue residue around the cDRA is 0.3 mm. Fig. 5 (c)-(d) show the variations obtained when the height of the glue and the horizontal alignment are varied, respectively. A degradation in the matching as well as a shift of several hundred MHz is observed. The sensitivity of these variations on the final response of the array can be observed in terms of the input reflection coefficient and the operating BW.

The far-field gain patterns as shown in Figs. 6 and 7, were measured using a calibrated anechoic chamber and a comparison between the simulated and measured values is provided. The 2D gain patterns at 30 GHz are shown in Fig. 6 where the beam is tilted towards the direction of interest. Similar results were observed at 31 GHz as well where the measurements and simulations are also in agreement (see Fig. 7). The small differences observed in the null values, SLL and positions are likely related to fabrication and assembly tolerances as previously described, as well as cable bending and twisting during the antenna measurements at mm-wave frequencies. For future work the SLL can be improved, which can be attributed to the small number of array elements as well as the beam tilting due to the feed network amplitude and phase imbalances and the presence of the compact GND plane.

The measured maximum realized gain values obtained were (6.9,8.6) dBi at 30 GHz, and (7.6,7.7) dBi at 31 GHz at the beam maximas for Port-1 and Port-2, respectively. Cross-polarization levels were less than 10 dB from the observed beam maximas. Note the clear beam tilt in the co-pol patterns. This can offer excellent channel isolation in the far-field which yields the low correlation coefficient. A dual-ridge horn (ETS-3116) antenna (18-40 GHz) was used in these 2D pattern measurements

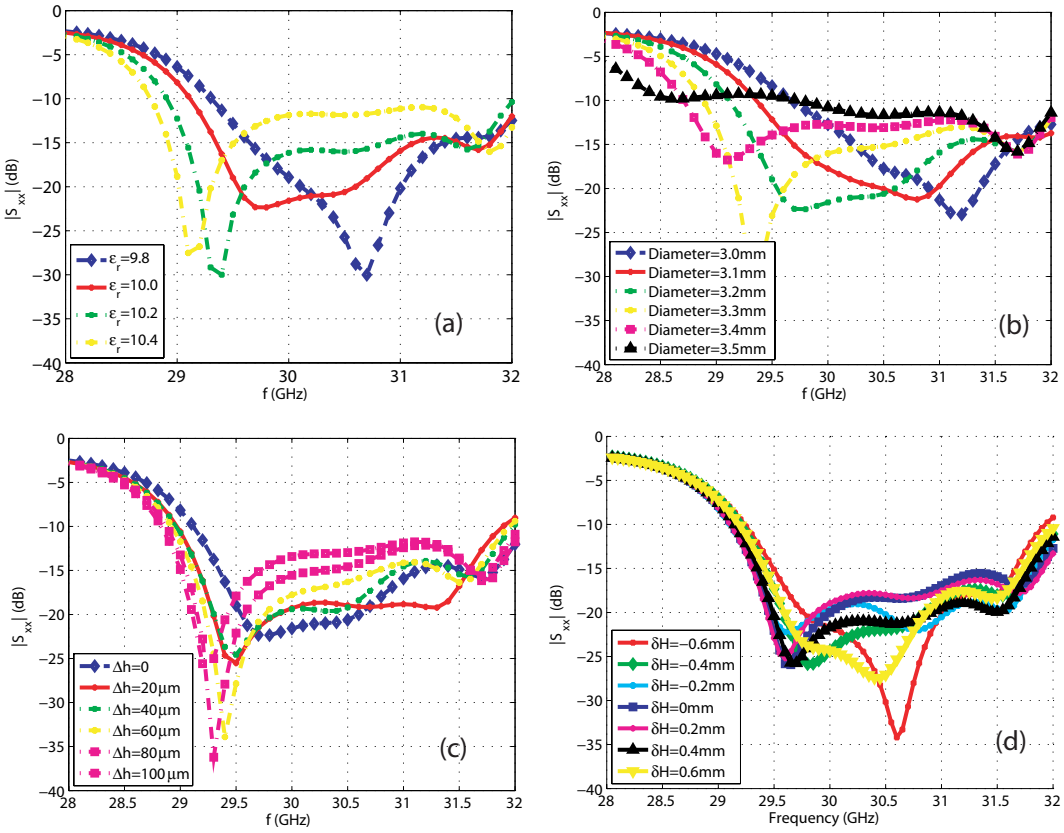

Fig. 5. Effect of fabrication parameters on the port reflection coefficient, (a) effect of ϵ_r variations (b) effect of glue residue diameter, (c) effect of glue height and (d) effect of horizontal shift placement.

in a far field anechoic chamber at the Royal Military College (RMC) of Canada. The gain substitution method was used. The maximum measured gain values for the two arrays across the operating band are shown in Fig. 8(a). The gain is slightly increasing at the higher operating bands. The obtained envelope correlation coefficient (ECC) values, ρ_e, based on the radiated far-fields as well as the measured S-parameters was very small (below 0.002, see Fig. 8(b)), which is desired for good MIMO operation [10]. Given these low ECC values, a diversity gain of 9.9 can be estimated at 30 GHz which is very close to the theoretical limit of 10 for an ideal, two-element MIMO antenna system. Without this beam tilting, the ECC would be much higher (also defining a reduction in the diversity gain) failing the requirements for good MIMO operation since both arrays will generate broadside beams that would overlap. Also, the simulated efficiency for the DRA array alone was 95%, while it dropped to 80% across the operating frequency when the feed system was included. The high efficiency of the cDRAs and the tilted beams justifies the close agreement between the port and field based ECC calculations.

Such a mm-wave cDRA based MIMO antenna can be very attractive for next generation wireless terminals due to its small form factor and good wideband performance for short range 4G/5G standards. Practically, the MIMO antenna system can be

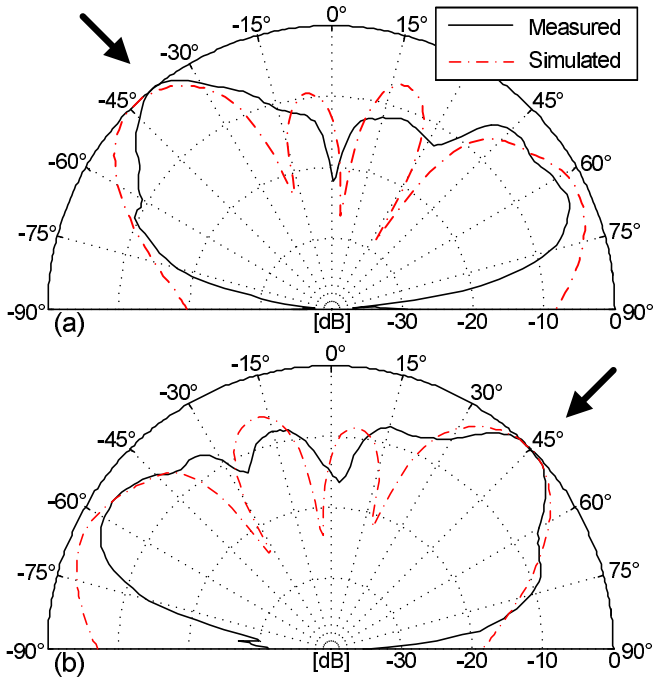

Fig. 6. Measured and simulated normalized 2D gain patterns for the MIMO antenna system at 30 GHz, (a) port 1, (b) port 2.

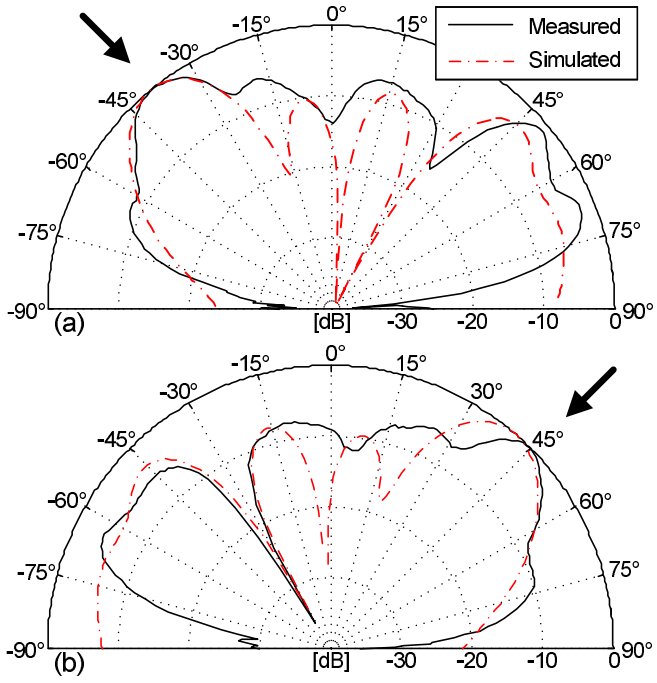

Fig. 7. Measured and simulated normalized 2D gain patterns for the MIMO antenna system at 31 GHz, (a) port 1, (b) port 2.

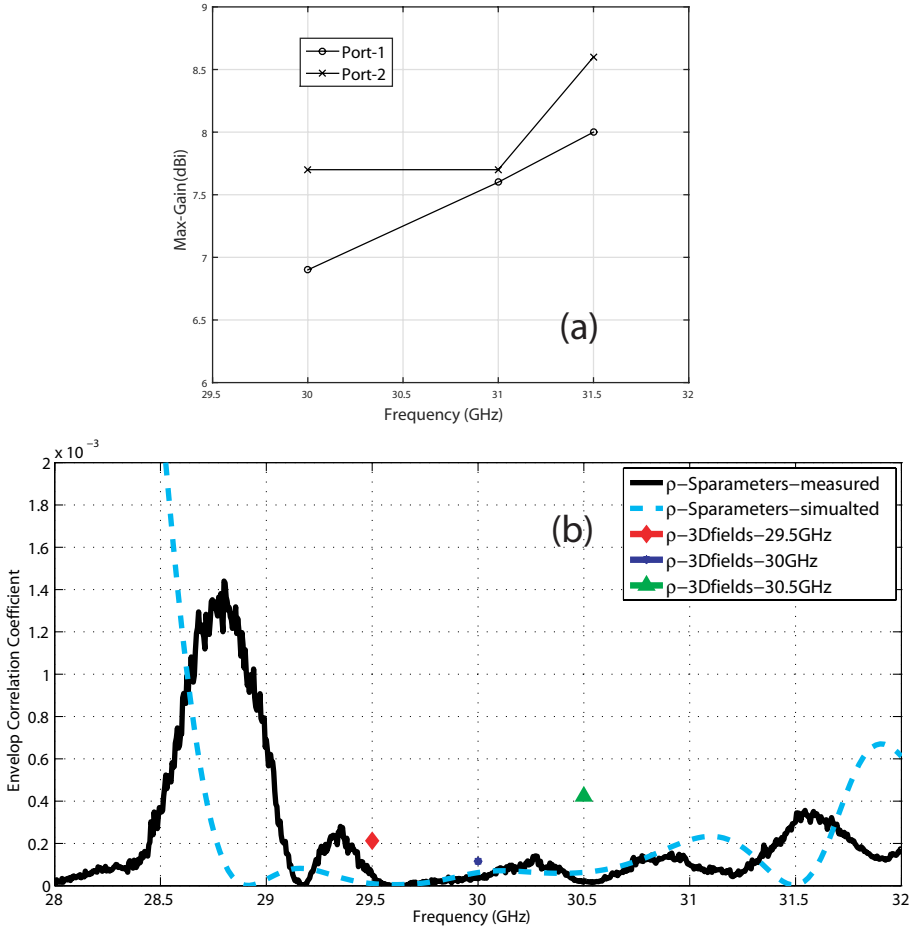

Fig. 8. (a) Maxim measured gain values as a function of frequency, (b) ECC (ρ_e) values from simulated 3D fields, and from the measured and simulated S-parameters.

integrated on the far top or bottom sides of a conventional 50×100 mm^2 mobile phone backplane, or on either top or bottom sides (quarter edge) of the same backplane.

IV. Conclusions

A mm-wave, MIMO antenna system based on cDRAs was proposed consisting of two, four-element linear cDRA arrays (eight-elements in total). A feeding network generates the two tilted beams which also provides the minimum field correlation coefficient. A maximum gain greater than about 7 dBi, including the feed network losses, was also obtained and an operating BW of at least 1 GHz was observed. The design is compact in size, efficient, and can fit on the edge of any commercial handheld device for short range high speed data links.

References

[1] A. Petosa, *Dielectric Resonator Antenna Handbook*, Artech House, 2007.

[2] K. M. Luk and K. W. Leung, *Dielectric Resonator Antennas*, Research Studies Press, 2003.

[3] R. K. Mongia and P Bhartia, "Dielectric Resonator Antennas A Review and General Design Relations for Resonant Frequency and Bandwidth," International Journal on RF and Microwave Computer Aided Engineering, Vol. 4, No. 3, pp. 230-247, July 1994.

[4] W. M. A. Wahab, D. Busuioc and S. S. Naeini, "Millimeter-Wave High Radiation Efficiency Planar Waveguide Series-Fed Dielectric Resonator Antenna (DRA) Array: Analysis, Design, and Measurements," *IEEE Transactions on Antennas and Propagation*, Vol. 59, No. 8, pp. 2834-2843, 2011.

[5] L. Ohlsson, T. Bryllert, C. Gustafson, D. Sjoberg, M. Egard, M. Arlelid and L. E. Wernersson, "Slot-Coupled Millimeter-Wave Dielectric Resonator Antenna for High-Efficiency Monolithic Integration," *IEEE Transactions on Antennas and Propagation*, Vol. 61, No. 4, pp. 1599-1607, 2013.

[6] M. G. Keller, M. B. Oliver, D. J. Roscoe, R. K. Mongia, Y. M. M. Antar and A. Ittipiboon, "EHF Dielectric Resonator Antenna Array," *Microwave and Optical Technology Letters, Wiley,*, Vol. 17, No. 6, pp. 345-349, 1998.

[7] M. T. Birand and R. V. Gelsthorpe, " Experimental Millimetric Array Using Dielectric Radiators Fed By Means Of Dielectric Waveguide," *Electronics Letters*, Vol. 17, No. 18, pp. 633-635, 1981.

[8] M. R. Nikkhah, J. R. Mohassel and A. A. Kishk, "Compact Low-Cost Phased Array of Dielectric Resonator Antenna Using Parasitic Elements and Capacitor Loading," *IEEE Transactions on Antennas and Propagation*, Vol. 61, No. 4, pp. 2318-2321, 2013.

[9] M. R. Nikkhah, J. R. Mohassel and A. A. Kishk, "High-Gain Aperture Coupled Rectangular Dielectric Resonator Antenna Array Using Parasitic Elements," *IEEE Transactions on Antennas and Propagation*, Vol. 61, No. 7, pp. 3905-3908, 2013.

[10] M. S. Sharawi, *Printed Antenna Engineering*, Artech House, 2014.

[11] -, "Printed Multi-Band MIMO Antenna Systems and Their Performance Metrics," *IEEE Antennas and Propagation Magazine*, Vol. 55, No. 5, pp. 218-232, October 2013.

[12] L. Huitema, M. Koubeissi, M. Mouhamadou, Eric Arnaud, C. Decroze and T. Monediere, "Compact and Multiband Dielectric Resonator Antenna With Pattern Diversity for Multistandard Mobile Handheld Devices," *IEEE Transactions on Antennas and Propagation*, Vol. 59, No. 11, pp. 4201-4208, 2011.

[13] R. Tian, V. Plicanic, B. K. Lau and Z. Ying, "A Compact Six-Port Dielectric Resonator Antenna Array: MIMO Channel Measurements and Performance Analysis," *IEEE Transactions on Antennas and Propagation*, Vol. 58, No. 4, pp. 1369-1379, 2010.

[14] J. B. Yan and J. T. Bernhard, "Implementation of a Frequency-Agile MIMO Dielectric Resonator Antenna," *IEEE Transactions on Antennas and Propagation*, Vol. 61, No. 7, pp. 3434-3441, 2013.

[15] T. S. Rappaport, S. Sun, R. Mayzus, H. Zhao, Y. Azar, K. Wang, G. N. Wong, J. K. Schulz, M. Samimi and F. Gutierrez, "Millimeter Wave Mobile Communications for 5G Cellular: It Will Work!," *IEEE Access*, Vol. 1, pp. 335 - 349, 2013.

[16] L. Huitema, et. al., "Compact and Multiband Dielectric Resonator Antenna With Pattern Diversity for Multistandard Mobile Handheld Devices," IEEE Transactions on Antennas and Propagation, Vol. 59, No. 11, pp. 4201-4208, 2011.

[17] P.Y. Qin, et. al., "A Pattern Reconfigurable U-Slot Antenna and Its Applications in MIMO Systems,"*IEEE Transactions on Antennas and Propagation*, Vol. 60, No. 2, pp. 516-528, 2012.

[18] D. Pozar *Microwave Enginering,* Fourth Edition, Wiley, 2011.

[19] C. Balanis, *Antenna Thoery: Analysis and Design,* Third Edition, Wiley, 2005.